Oxidation of Cyclic Dipeptides by Photoinduced H-Atom Abstraction. A Laser Flash FT EPR and Optical Spectroscopy Study

Peter Tarábek,[†] Marija Bonifačić,*[,‡] and Dieter Beckert*[,†]

Interdisciplinary Research Group "Time Resolved Spectroscopy", Faculty of Chemistry and Mineralogy, University of Leipzig, Permoserstrasse 15, Leipzig, D-04318, Germany, and Department of Physical Chemistry, Ruđer Bošković Institute, Bijenička c. 54, HR-10 000 Zagreb, Croatia

Received: February 5, 2007; In Final Form: March 27, 2007

Laser flash photolysis with the Fourier transform electron paramagnetic resonance (FT EPR) and optical spectroscopy detection methods on the nanosecond time scale have been employed in order to investigate the oxidation mechanism of cyclic dipeptides glycine, alanine, and sarcosine anhydrides initiated by $SO_4^{\bullet-}$ or 9,10-anthraquinone-2,6-disulfonate (2,6-AQDS) triplet in oxygen free aqueous solutions. A direct hydrogen abstraction from the ring C−H position of an anhydride by both oxidants is proposed as the primary reaction, rather then an electron transfer from nitrogen followed by $^{\alpha}$C−H deprotonation. The overall second-order rate constants for the reaction with $SO_4^{\bullet-}$ were determined to be 7.2×10^7 M^{-1} s^{-1}, 1.2×10^8 M^{-1} s^{-1}, and 5.2×10^8 M^{-1} s^{-1} for glycine anhydride, alanine anhydride, and sarcosine anhydride, respectively. The rate constants for 2,6-AQDS triplet as oxidizing species are about two times lower. The radical intermediate products derived from cyclic dipeptides observed on the microsecond time scale were assigned to the general structure of piperazine-2,5-dione-3-yl radical. These are spin polarized by the mechanisms of chemically induced dynamic electron polarization (CIDEP). For $SO_4^{\bullet-}$ as the oxidant the spectra are exhibiting an E/A* polarization pattern originating partially from F-pairs of two piperazine-2,5-dione-3-yl radicals.

1. Introduction

Damage of proteins induced by oxidation processes is considered to be responsible for essential changes in biological systems with significant biochemical, medical, and industrial consequences. In the course of this, the α-C-centered peptide radicals (−NH−C$^{\bullet}$R−CO−) have been suggested to play an important role in protein−DNA cross-linking,[1,2] protein degradation, and fragmentation,[3] but also as species involved in the catalytic activity of some enzymes.[4,5] The α-C-centered peptide radicals can be formed via hydrogen abstraction from the C−H bonds of the (poly)peptide chain. However, oxidation of peptides and proteins leading to the same intermediates can also be initiated by an electron-transfer mechanism. Both primary reactions, hydrogen and electron transfer, can in principle take place also on easy to oxidize side groups, e.g., on the thiol group in cysteine, on the phenol group of tyrosine, or at the C/N end of the (poly)peptide.[6] The $-^{\alpha}$C$^{\bullet}$R− radicals are stabilized by captodative effects,[7,8] which lower also the bond dissociation enthalpy (BDE) of the parent molecule $^{\alpha}$C−H bond.[9] According to the quantum-chemical calculations, the latter is a very weak bond in the range of 330−370 kJ mol^{-1} for all amino acid residues.[10,11] For comparison, BDE($^{\alpha}$C−H, 2-propanol) = 393.2 kJ mol^{-1};[12] BDE(S−H, thiols) ca. 370 kJ mol^{-1}.[13] Similar calculations for glycine and alanine anhydrides yielded BDE($^{\alpha}$C−H) of 351 and 335 kJ mol^{-1}, respectively.[6] Under laboratory conditions the hydrogen atom abstraction by $^{\bullet}$OH, O$^{\bullet-}$, or H$^{\bullet}$ radicals generated by radiolysis of water has been the most common method for generation of the peptide $-^{\alpha}$C$^{\bullet}$R− radicals.[14−18] The use of other methods has been reported as well.[19−21] Cyclic dipeptides (diketopiperazines, amino acid anhydrides) have been often used in radiation-chemical[22−25] and photochemical investigations[26,27] as model compounds for the peptide backbone. The advantage of amino acid anhydrides is in the nonexistence of the terminal peptide functional groups and the effects arising thereof. However, the question if they really can serve as good models is not easy to answer, since their geometrical structure and the chemical properties connected with it differ from those found in open chain aliphatic peptides,[28,29] *e.g.*, the peptide linkages (−CONH−) in cyclic dipeptides have a *cis* configuration, whereas the preferred configuration in an open chain aliphatic peptide is *trans*.[30] The thermodynamic properties of cyclic dipeptides and their role as protein model compounds have been discussed as well.[31,32] In recent years the biological importance of over one hundred diketopiperazines found in nature has been demonstrated.[33] It has been shown that not only do they appear as byproducts of fermentation and food processing but also they are endogenous to animals and plants exhibiting different kinds of biological activity.[33−35]

In spite of rather numerous previous investigations, cyclic peptides still remain a relatively unexplored class of compounds. Concerning chemical and physicochemical data about radicals derived from cyclic dipeptides, the information in the literature is restricted mostly to pulse radiolysis investigations and theoretical studies.[6,9,18,23,36−38] There is only spare information from EPR experiments.[24,25] This motivated us to contribute to this interesting topic. The current paper presents the results obtained from laser flash photolysis experiments with Fourier transform EPR and optical detection of oxygen-free aqueous solutions containing $K_2S_2O_8$ or anthraquinone-2,6-disulfonate disodium salt (2,6-AQDS) in the presence of cyclic dipeptides

* Corresponding authors. E-mail: beckert@mpgag.uni-leipzig.de (D.B.); bonifacic@irb.hr (M.B.).
[†] University of Leipzig.
[‡] Ruđer Bošković Institute.

10.1021/jp0709914 CCC: $37.00
Published on Web 05/22/2007

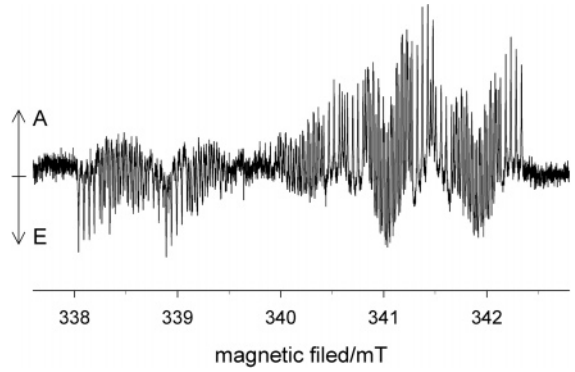

Figure 1. FT EPR spectrum of radical **1** measured 4 μs after laser pulse irradiation in an aqueous solution of 0.1 M $K_2S_2O_8$ and 0.1 M glycine anhydride at pH ~3.

glycine, alanine, or sarcosine anhydride. Primary reactive species formed upon laser flash photolysis were $SO_4^{\bullet -}$ or 2,6-AQDS triplet, both strong oxidizing agents.[39,40] Structural and kinetic data of radical intermediates produced in their reaction with the cyclic dipeptides have been obtained.

2. Experimental Section

A KrF excimer laser (ATL Lasertechnics & Acc. Ltd., ATLEX-SP-25) with 248 nm radiation wavelength, pulse energy 1−10 mJ, and 3 ns pulse duration was used for photoexcitation in FT EPR experiments. The FT EPR setup has been described previously.[41,42] The power of the microwave pulse used in the experiments was 1 kW with a pulse length for the $\pi/2$ pulse of 16 ns. The excitation width in the spectra was thus about $\Delta B = \pm 1.5$ mT. Complete spectra were therefore obtained by changing the magnetic field offset and putting partial spectra together using suitable graphing software. The resonant cavity was the Bruker split-ring module ER 4118X-MS-5W. The receiver dead time took 80−100 ns from the FID. All experimental FID data were extrapolated using the linear prediction singular value decomposition method (LPSVD).[43,44] While using the LPSVD extrapolation method one must be always aware of the limitations of its performance. A slight uncertainty in setting the zero point (end of the microwave pulse) may cause some distortion of the Fourier-transformed signal, particularly of the baseline of a spectrum (*cf.* Figure 1). Problems may occur especially if the S/N ratio is low and/or with a high density of lines.[45]

The Fourier-transformed EPR spectra have been simulated using the Bruker WIN-EPR SimFonia software.

For the time-resolved optical experiments, solutions were photolyzed by the third and fourth harmonics (355 and 266 nm) of a Quanta-Ray GCR-11 Nd:YAG laser (Spectra Physics). Pulses of ≤3 ns duration (fwhm) with energies of up to 5 mJ were used. The optical detection system consisted of a pulsed xenon lamp (XBO 450, Osram), a monochromator (SpectraPro 275, Acton Research), a R955 photomultiplier tube (Hamamtsu Photonics), and a 500 MHz digitizing oscilloscope (DSA 602 A, Tektronix). The laser power was monitored for every pulse using a bypass with fast Si photodiode.

Potassium peroxodisulfate ($K_2S_2O_8$, Fluka), anthraquinone-2,6-disulfonic disodium salt (2,6-AQDS, Aldrich), sarcosine anhydride (Acros), and alanine anhydride (Aldrich) were used as received. Glycine anhydride (Acros) was recrystallized from water. Water was taken from a milli-Q plus ultrapure water system (Millipore). Deuterium oxide (99.8%) from Deuchem GmbH (Leipzig) was used for measurements with D_2O as solvent.

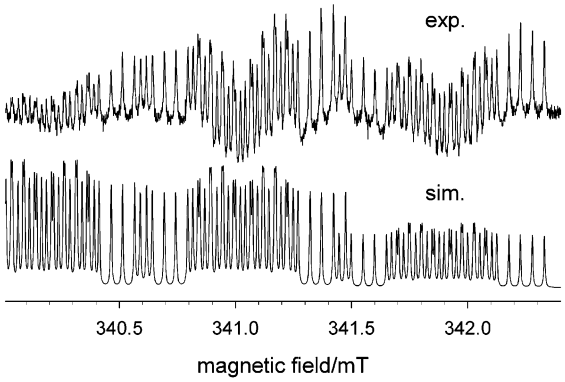

Figure 2. High field part of the spectrum from Figure 1 with corresponding simulation. For details see text and Table 1.

CHART 1: Cyclic Peptide Radical Structures

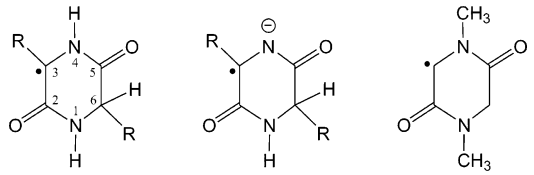

1 : R = H
2 : R = CH_3

1a : R = H
2a : R = CH_3

3

The solution flowed through the EPR tube (optical path length about 1.0 mm) at a rate of about 5 mL/min to avoid depletion of the sensitizer and/or enrichment of reaction products. A flowing system was also used in optical experiments. Solutions were prepared without adding any buffer. Whenever necessary, pH was adjusted by KOH (Aldrich). To remove oxygen, the samples were bubbled with argon or nitrogen before (about 20 min) and during the whole experiment. In order to improve the S/N ratio, each signal was averaged (with a number of accumulations 1000−4000 for EPR and 1−5 for optical measurements). All measurements were carried out at room temperature.

3. Results and Discussion

3.1. Cyclo(Gly-Gly) Peptide Radical. The FT EPR spectrum shown in Figure 1 was recorded 4 μs after the laser pulse irradiation of an aqueous solution containing 0.1 M $K_2S_2O_8$ and 0.1 M cyclo(Gly-Gly) at pH ~3. The high field part of the spectrum is again depicted in Figure 2 together with its simulation. The spectrum is attributed to the piperazine-2,5-dione-3-yl radical **1** (Chart 1). The simulation parameters are listed in Table 1 and are in very good agreement with those determined by Taniguchi and Kirino.[24] In order to verify the assignment of the coupling constants of hydrogen atoms bound to nitrogen, experiments in D_2O have been carried out (spectra not shown, *cf.* Table 1). The spectrum in H_2O consists of 216 lines from which about 170 could be detected and separated. The rest of the lines, located in the central part of the spectrum, is undetectable because of CIDEP effects (see below for explanation). The large number of lines indicates a strong delocalization of the unpaired electron within the cyclic peptide radical in comparison to the corresponding linear peptide radical.[20,46] Apart from this, the lines are also remarkably narrow with a line width of only about 5 μT (2 μT in D_2O). The detection and separation of so narrow and numerous lines have been achieved due to the high magnetic field stability of the instrument, as well as the relatively long lifetime of the measured species. Namely, in the investigated solution it is reasonable to

TABLE 1: Hyperfine Coupling Constants *A* and *g* Factors for Radicals Derived from Cyclic Dipeptides[a]

radical	A_{N1}	A_{N4}	$A_{H/D/CH_3(N1)}$	$A_{H/D/CH_3(N4)}$	$A_{H/CH_3(C3)}$	$A_{H(C6)}$	$A_{CH_3(C6)}$	*g* value
1	0.052	0.153	0.227	0.248	1.713	0.856 (2)		2.00339
in D_2O	0.047	0.150	0.036	0.039	1.713	0.856 (2)		2.00342
1a	0.055	0.158	0.215		1.477	1.243 (2)		2.00345
2	0.023	0.155	0.163	0.235	1.742 (3)	0.800	0.023 (3)	2.00342
in D_2O	0.024	0.152	0.026	0.037	1.746 (3)	0.799	0.024 (3)	2.00344
2a	0.036	0.185	0.155		1.460 (3)	0.950	0.036 (3)	2.00335
3	0.067	0.205	0.181 (3)	0.275 (3)	1.691	0.934 (2)		2.00339

[a] In parentheses, the number of equivalent protons is shown. The hyperfine constants are given in mT and are acurate to ±0.002 mT. The *g* factors were obtained relative to the spectrum of 2,6-AQDS anion radical with $g = 2.00412$[41] and are accurate to about ±0.00002.

SCHEME 1

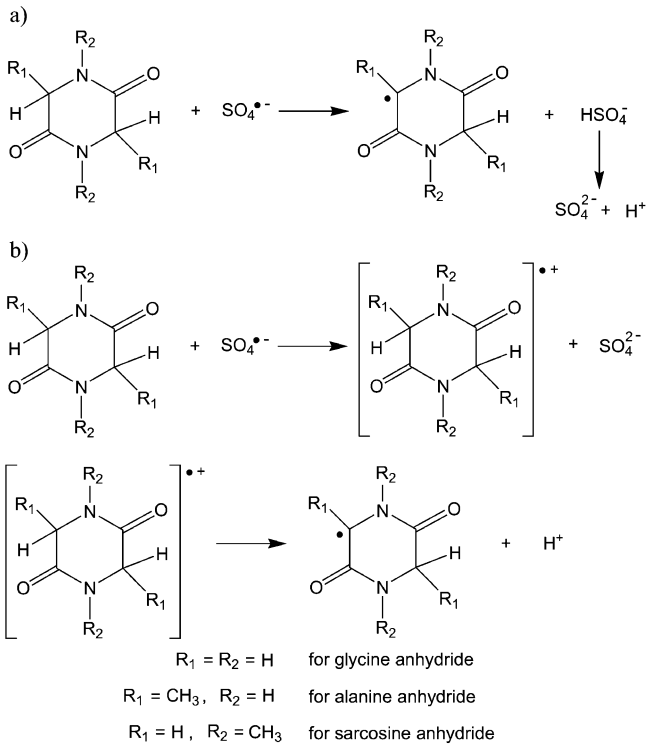

assume that radical **1** decays only by the second-order radical−radical self-termination reaction ($k(\mathbf{1}+\mathbf{1}) = 7.0 \times 10^8$ M^{-1} s^{-1})[18] and that its reactions with the parent cyclo(Gly-Gly) and/or $S_2O_8^{2-}$ are negligible.

Generation of the cyclic peptide radical **1** is ascribed to the reaction of glycine anhydride with $SO_4^{\bullet-}$ radical anion. The latter has been formed by the photodissociation of peroxodisulfate $S_2O_8^{2-}$, which occurs by the O−O bond scission upon laser light excitation. Sulfate radical anion is a strong oxidation agent with $E^0(SO_4^{\bullet-}/SO_4^{2-}) = 2.4$ V[47] and is known to react with many compounds by electron transfer[48] but can also directly abstract an H atom, as it has been suggested for oxidation of alkanes, ethers, alcohols, or carbohydrates.[49] Because of exceptionally low BDE values for cyclic dipeptides' $^{\alpha}$C−H bonds (*cf.* Introduction) as well as a relatively high ionization energy reported for the peptide bond,[50] a direct hydrogen atom abstraction, Scheme 1a, seems to us to be the more likely mechanism of radical **1** formation. The other possibility would be an electron transfer followed by the proton loss from the $^{\alpha}$C−H position, Scheme 1b. Deprotonation of the radical cation intermediate from the N−H group would lead to the nitrogen centered radical. We have found no experimental evidence (characteristic EPR signals) for such a radical presence.

The reaction of $SO_4^{\bullet-}$ with cyclic dipeptides was in this study kinetically followed by laser flash photolysis with optical detection, and the rate constants are listed in Table 2. For comparison the quenching rate constants of the 2,6-AQDS triplet have been obtained by the same method and are also listed in Table 2. The 2,6-AQDS triplet is considered to react with investigated cyclic dipeptides in the same way as the sulfate radical anion, i.e., by an H-atom abstraction mechanism followed by deprotonation of 2,6-AQDSH$^{\bullet}$ formed in the reaction (*cf.* Scheme 1a).

TABLE 2: Measured Overall and Calculated per $^{\alpha}$C−H Bond Rate Constants for Cyclic Dipeptide Oxidation with Sulfate Radical Anion and 2,6-AQDS Triplet in Aqueous Solutions[a]

	$k(SO_4^{\bullet-})$		$k(2,6\text{-AQDS}_T)$	
reactant	overall	per $^{\alpha}$C−H	overall	per $^{\alpha}$C−H
cyclo(Gly-Gly)	7.16 ± 0.06	1.8	3.6 ± 0.2	0.9
cyclo(Ala-Ala)	12.0 ± 0.1	6.0	6.8 ± 0.1	3.4
cyclo(Sar-Sar)	52 ± 1	13.0	21.3 ± 0.3	5.3

[a] Units: 10^7 M^{-1} s^{-1}.

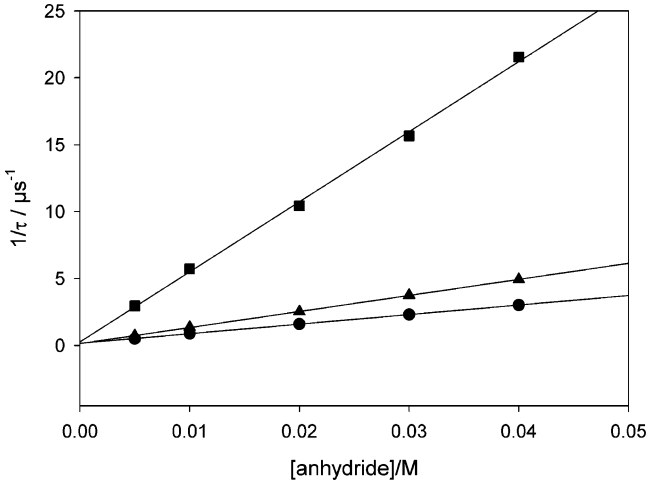

Figure 3. Decay rates of $SO_4^{\bullet-}$ species determined by time-resolved optical spectroscopy at 455 nm versus anhydride concentration. Samples: 75 mM $K_2S_2O_8$, pH ~3. Legend: ●, glycine anhydride; ▲, alanine anhydride; ■, sarcosine anhydride.

After laser (266 nm) flash photolysis of $K_2S_2O_8$ containing solutions, the decay kinetics of $SO_4^{\bullet-}$ radical absorption monitored at 455 nm was measured as a function of different cyclic dipeptide concentrations. The decay was always exponential and accelerated with increasing cyclic dipeptide concentration. The experimentally obtained overall second-order rate constants, $k(SO_4^{\bullet-})$, were determined from the slopes of the respective Stern−Volmer plots (Figure 3). With the 2,6-AQDS triplet sensitizer the kinetics of the triplet quenching has been monitored at 380 nm. Other details concerning the 2,6-AQDS triplet deactivation kinetics have been reported elsewhere.[51] The obtained Stern−Volmer plots and corresponding overall second-order quenching rate constants, $k(2,6\text{-AQDS}_T)$, are shown in Figure 4 and Table 2, respectively (error limits in

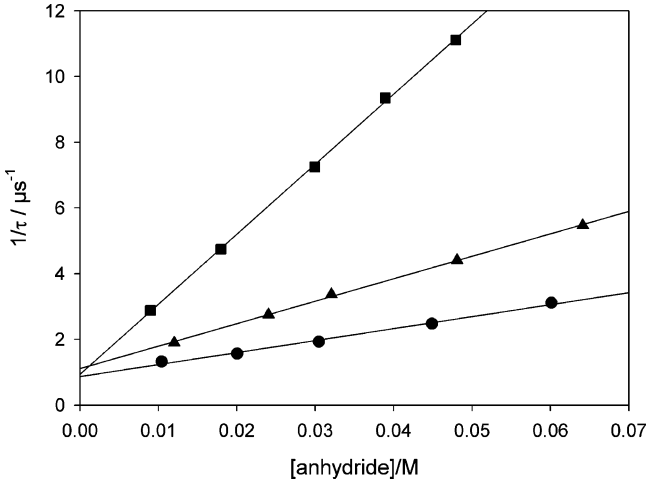

Figure 4. Decay rates of 2,6-AQDS triplet determined by time-resolved optical spectroscopy at 380 nm versus anhydride concentration. Samples: 0.2 mM 2,6-AQDS, pH ~10. Legend: ●, glycine anhydride; ▲, alanine anhydride; ■, sarcosine anhydride.

Table 2 refer only to the least-squares fits of the experimental data). Table 2 contains also rate constants calculated per $^{\alpha}C-H$ available (glycine and sarcosine anhydride have four such groups, and there are only two in the case of alanine anhydride). The rate constants obtained increase in the order glycine, alanine, and sarcosine anhydride as reactants with both oxidizing agents, revealing the sulfate radical anion to be the more efficient one. Compared with glycine anhydride, the rate constant per $^{\alpha}C-H$ increases for alanine anhydride by a factor of 3.5 in average for the two oxidants. This is in good correlation with the corresponding BDE($^{\alpha}C-H$) values (351 and 335 kJ mol^{-1},[6] for the two anhydrides, respectively). For sarcosine anhydride, with the methyl substituent on nitrogen, the increase is even more pronounced and amounts to a factor of 7.2 for $SO_4^{\bullet-}$ and 5.9 for 2,6-AQDS triplet.

Radical **1** has been confirmed as the main product in the reaction of $SO_4^{\bullet-}$ with cyclo(Gly-Gly) by measuring the transient optical spectra from the recorded time profiles at different wavelengths in the range of 300−550 nm. Thus, at the time immediately after the laser pulse the spectrum belonged solely to $SO_4^{\bullet-}$ ($\lambda_{max} = 450$ nm, $\epsilon_{450} = 1100$ M^{-1} cm^{-1}).[52] As this species decayed, another absorption was formed with the same rate showing a maximum at 365 nm characteristic for radical **1** ($\epsilon_{365} = 1760$ M^{-1} cm^{-1}).[18] A ratio of the optical densities measured at 455 nm 0.04 μs and at 365 nm 2.5 μs after the laser pulse, that is, at the time of maximum $SO_4^{\bullet-}$ concentration and after its conversion into radical **1** was completed, amounted to 0.845 in a solution containing 40 mM $S_2O_8^{2-}$ and 40 mM cyclo(Gly-Gly), pH 3. Taking the ratio of the two species molar absorption coefficient of 1100/1760 = 0.625, the transformation of $SO_4^{\bullet-}$ into radical **1** has been calculated to occur with 74% efficiency. This confirms radical **1** as the major reaction product. Considering certain inaccuracy of the molar absorption coefficients used and because there was no indication of the presence of other radicals in the EPR spectra obtained in the same systems, it might as well be that radical **1** was the only radical produced in the reaction. Similar results were obtained for alanine anhydride.

Figure 5 represents the low field part of an FT EPR spectrum measured in a solution containing 0.5 mM 2,6-AQDS, 125 mM cyclo(Gly-Gly) at pH 11.7, recorded 0.4 μs after the laser pulse. The spectrum was simulated with parameters given in Table 1 and was attributed to the deprotonated form of radical **1**, *i.e.*, radical **1a** in accordance with ref 24. The anion radical derived

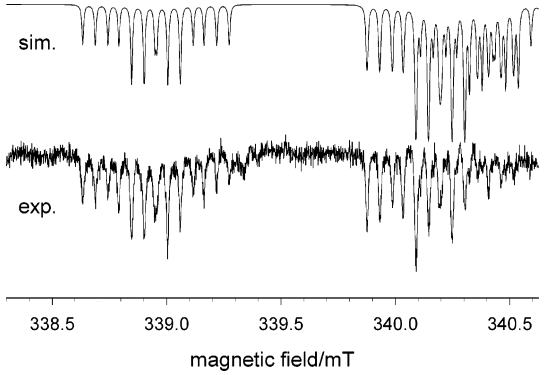

Figure 5. Low field part of experimental and simulated spectra of radical **1a** obtained in a system of 0.5 mM 2,6-AQDS, 125 mM glycine anhydride at pH 11.7; delay time 0.4 μs. The simulation parameters are listed in Table 1.

from 2,6-AQDS was also observed as a product, formed after deprotonation of 2,6-AQDSH$^{\bullet}$ successor radical generated during the hydrogen abstraction reaction (*cf.* Scheme 1a). Its EPR spectrum appears beyond the range shown on Figure 5 and, together with details of its structure, will not be further discussed in this study.[41,53] The effect of cyclization and resonance delocalization shifts the dissociation of NH protons in cyclic peptide radicals to less basic solutions compared to the linear peptide radicals.[24] Thus, the pK_a value of the −NHCO− group adjacent to $-^{\alpha}C^{\bullet}R-$ in the case of cyclo(Gly-Gly) radical **1** has been reported to be 9.8.[16,18] The reason for the use of 2,6-AQDS photosensitizer instead of peroxodisulfate in the experiment at higher pH is the decay of $SO_4^{\bullet-}$ due to reaction 1.

$$SO_4^{\bullet-} + OH^- \rightarrow SO_4^{2-} + {}^{\bullet}OH \quad (1)$$

$$SO_4^{\bullet-} + H_2O \rightleftharpoons {}^{\bullet}OH + SO_4^{2-} + H^+ \quad (2)$$

The interconversion of $SO_4^{\bullet-}$ to $^{\bullet}$OH radical is known to occur even in neutral and acidic solutions, reaction 2,[54−56] however with a rate constant of only 10^3-10^4 M^{-1} s^{-1}, which value is over 3 orders of magnitude lower than the rate constant of reaction 1.[52,57] Formation of hydroxyl radicals at pH ≤ 7 could be thus neglected under our experimental conditions but might interfere at higher pHs.

3.1.1. Polarization Patterns and Mechanisms. The appearance of the spectrum of radical **1** in Figure 1 is influenced by the CIDEP effect,[58] exhibiting an E/A* pattern, where the asterisk denotes a preponderance. In order to understand the formation and behavior of spin polarization in the investigated system, we have to look at the sequence of elementary physical and chemical events in the course of reaction leading to the formation of spin polarized radical **1**. The sulfate radical $SO_4^{\bullet-}$ is supposed to be generated in a nonpolarized state, the peroxide dissociating through the excited singlet state.[59] Nevertheless it should exist initially as a part of a geminate radical pair $[SO_4^{\bullet-}\cdots SO_4^{\bullet-}]$. However, such a radical would give only one line (no hyperfine coupling), and therefore no spin polarization can be possibly created in the geminate radical pair $[SO_4^{\bullet-}\cdots SO_4^{\bullet-}]$. In addition, sulfate anion radicals have never been observed by direct EPR techniques at room temperature, because of their fast spin−spin and/or spin−lattice relaxation,[57] and so it was also in the presented study. Radical **1** is formed *via* simple radical transfer, Scheme 1a, during which no polarization can be transmitted to radical **1**, since sulfate anion radical is nonpolarized. The only possibility for creation of polarization

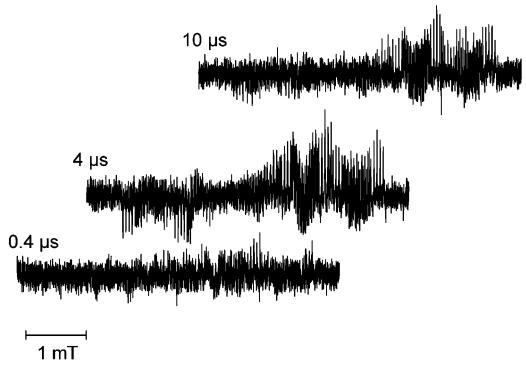

Figure 6. FT EPR spectrum of radical **1** measured at three different time delays: 0.4 μs, 4 μs, and 10 μs after laser pulse in a solution of 0.1 M $K_2S_2O_8$ and 0.1 M glycine anhydride at pH ~3.

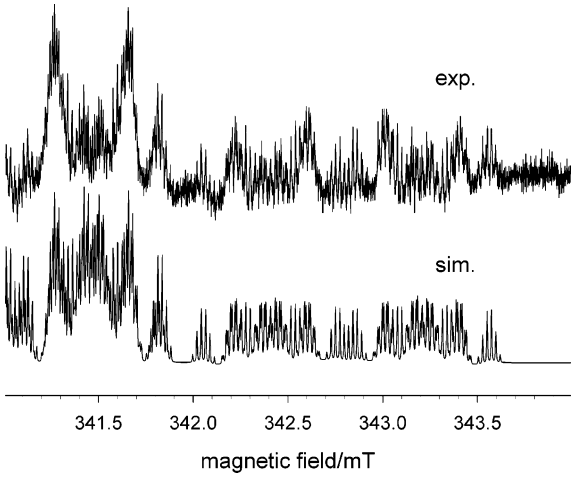

Figure 7. High field lines of experimental and simulated spectra of radical **2**. Sample: 0.1 M $K_2S_2O_8$, 0.1 M alanine anhydride at pH ~3; delay time 4 μs. The simulation parameters are listed in Table 1.

for the cyclic peptide radicals is within a "freely-diffusing correlated pair (F-pair)". The term F-pair has been introduced in order to distinguish it from the geminate spin-correlated pair which is formed in the primary process of radical generation. F-pairs are produced by encounter of radicals originating from separate formation events. As the radicals diffuse together, they experience the electron exchange interaction and become spin-correlated.[60] The sulfate anion radical can be excluded as a counter partner to create F-pair polarization[61] with radical **1** because (a) at the time of observation of polarized radical **1** (maximal intensity at 4 μs) there is practically no $SO_4^{\bullet-}$ present in the solution ($\tau(SO_4^{\bullet-}) = 14$ ns at concentration of cyclo-(Gly-Gly) 0.1 M) and (b) its participation in any radical pair would destroy polarization by an effective relaxation mechanism, similarly as it is in the case of hydroxyl radicals.[62,63] The presence of another suitable radical in the solution, which might create, together with the cyclic peptide radical **1**, radical pair polarization (RPP) with the E/A* pattern is rather unlikely. Therefore, the only counter partner can be the cyclic peptide radical itself.

The necessary condition for the F-pair polarization to be observed is a termination reaction which removes some of the radical pairs (those in the singlet state) from the system. Otherwise, equal but opposite polarizations in the radicals coming from equal numbers of S (singlet) and T_0 (triplet) pairs would yield a zero resultant.[60] Indeed, cyclic peptide radicals tend to form dehydrodimers with a second-order rate constant of $\sim 5 \times 10^8$ M^{-1} s^{-1}.[18] If the pair is at the moment of encounter in the triplet state, the radicals undergo spin mixing and generate spin polarization. After they escape the radical pair and diffuse apart, they can be observed by FT EPR, unless their relaxation and/or transformation to other species are not faster than the time resolution of the technique used. In general, the F-pair polarization is generated for as long as reactive radicals persist in the system.[60] This could be documented also in the case of radical **1**, Figure 6, where at the time of 10 μs there is still some RPP observable.

Since in the case of radical **1** in the investigated system the RPP with the E/A* pattern cannot originate from a pair with two different radical species with different *g* values, we need to consider the line intensities as a sum of two quite separate contributions. One is of a single phase, in absorption, originating in general either from spin-polarized or from relaxed radicals. McLauchlan et al. have provided a full discussion concerning this single phase part based on comprehensive study of propan-2-olyl radical CIDEP spectra.[59] The second contribution, with multiple phase line intensities, results from the radical pair mechanism and has the characteristic form that the low and high field parts of the spectrum are in the opposite phase. As mentioned above this contribution originates from the F-pair RPP. However, the FT EPR time profile of radical **1** is rather complicated to analyze quantitatively because of many influencing factors including generation of radical **1**, its decay by dehydrodimer formation and creation of F-pair polarization as well as the single-phase contribution and spin−lattice relaxation to thermal equilibrium. Those different processes are difficult to separate in the experimental time domain. That was also the reason why the rate constants of the hydrogen abstraction by sulfate radical anion and 2,6-AQDS triplet were measured by laser flash photolysis with optical detection.

3.2. Cyclo(Ala-Ala) Peptide Radical. The laser pulse irradiation of an aqueous solution containing 0.1 M $K_2S_2O_8$ and 0.1 M cyclo(Ala-Ala) at pH ~3 has resulted in the formation of radical species whose FT EPR spectrum (high field lines) is shown in Figure 7. The simulation has been carried out with parameters listed in Table 1. In accordance with the discussion above, the spectrum was assigned to the structure of 3,6-dimethylpiperazine-2,5-dione-3-yl radical, **2**. In basic solutions (pH >11) with 2,6-AQDS triplet as oxidizing agent the deprotonated form, radical **2a**, could be detected (spectrum not shown). The pK_a value of radical **2** has been reported to be 10.6, which is significantly higher than that of radical **1** because of the electron-donating effect of the α-methyl group increasing the electron density at the adjacent carbon and hence impeding the deprotonation at the neighboring nitrogen.[18] The EPR hyperfine coupling constants of the deprotonated radical **2a** are also listed in Table 1. The above discussion concerning the polarization mechanisms and reactions of cyclo(Gly-Gly) peptide radical formation as well as radical−radical termination is applicable also for cyclo(Ala-Ala) radical.

3.3. Cyclo(Sar-Sar) Peptide Radical. As for cyclo(Gly-Gly) and cyclo(Ala-Ala) the sulfate radical is able to abstract hydrogen atom from the $^{\alpha}$C−H bond also in the case of the cyclo(Sar-Sar) molecule. The FT EPR spectrum (high field lines) of the corresponding cyclic peptide radical **3** is displayed in Figure 8 together with its simulation (for simulation parameters see Table 1). The spectrum was recorded 4 μs after a laser pulse in a solution containing 0.1 M $K_2S_2O_8$ and 0.1 M cyclo(Sar-Sar) at pH ~3. It shows the characteristic E/A* polarization pattern. Using $^{\bullet}$OH radical as the oxidation agent, Mieden and von Sonntag[18] detected also a radical formed by the direct H-atom abstraction from one of the methyl groups bound at nitrogen with a yield of about 20%. Such a radical could not

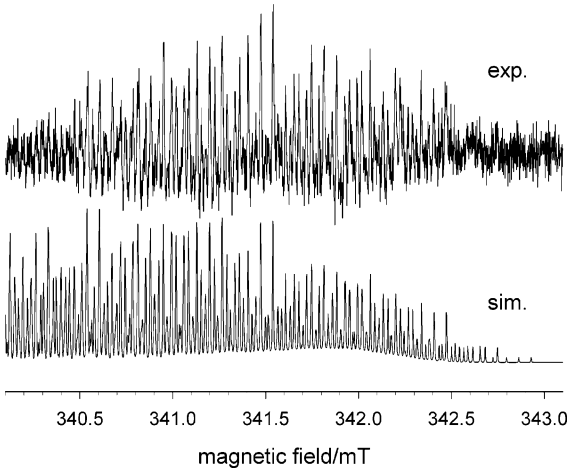

Figure 8. High field part of experimental and simulated spectra of radical **3**. Sample: 0.1 M $K_2S_2O_8$, 0.1 M sarcosine anhydride at pH ~3; delay time 4 μs. The simulation parameters are listed in Table 1.

be detected in our study, most probably because of higher selectivity of $SO_4^{\bullet-}$ radical.

It has to be emphasized at this point, however, that, in contrast to the other two anhydrides, in the systems with sarcosine anhydride the incidental laser light is mostly absorbed by the anhydride and not by $S_2O_8^{2-}$, since its molar absorption coefficient at 248 nm is about 5 times higher than that of persulfate. Still, the FT EPR spectrum of radical **3** resulting from the experiment with equal amounts (0.1 M) of $K_2S_2O_8$ and cyclo(Sar-Sar), pH ~3, exhibits approximately the same polarization pattern and line intensities as the spectra of radicals **1** and **2** formed in solutions where the laser light is absorbed directly by persulfate. This phenomenon could be explained by an energy transfer from the primarily formed triplet excited state of cyclo(Sar-Sar) to the persulfate molecule which consecutively dissociates into two sulfate radicals. Experiments are in progress in order to explore the role of sarcosine anhydride as a triplet sensitizer.

4. Conclusions

The transients $SO_4^{\bullet-}$ and 2,6-AQDS triplet formed after photolysis of deoxygenated aqueous solutions of $K_2S_2O_8$ or 2,6-AQDS, respectively, have been found to be efficient oxidation agents toward cyclic dipeptides glycine anhydride, alanine anhydride, and sarcosine anhydride. The reactions lead to the formation of piperazine-2,5-dione-3-yl type radicals as the first observed transients. This has been shown by time-resolved FT EPR spectroscopy measurements. A direct hydrogen atom abstraction from the anhydride $^{\alpha}$C−H position is proposed as the most likely reaction mechanism. The overall rate constants for $SO_4^{\bullet-}$ radical are about 2 times higher than the rate constants for 2,6-AQDS triplet quenching as determined by time-resolved optical measurements. They amount to 7.2×10^7, 1.2×10^8, and 5.2×10^8 M^{-1} s^{-1} for the reaction of $SO_4^{\bullet-}$ with glycine, alanine, and sarcosine anhydride, respectively. For alanine anhydride, comparing with glycine anhydride, this is an increase by a factor of 3.3 per available $^{\alpha}$C−H bond, in accordance with the lower $^{\alpha}$C−H BDE of the former compound. Further increase by a factor of 7.2 per available $^{\alpha}$C−H bond measured for sarcosine anhydride is to be ascribed to the methyl substitution at nitrogen which is increasing the electron density at α-carbon and thus making the $^{\alpha}$C−H bond even weaker.

The number of lines observed in the FT EPR spectra of cyclic peptide radicals **1**, **2**, and **3** reveals a high delocalization of the unpaired electron within the radical. Analyzing the polarization patterns of the FT EPR spectra it has been concluded that the E/A* pattern can be interpreted as a sum of two contributions: an E/A multiple phase caused by ST_0 radical pair mechanism and an absorptive single phase, originating from relaxed radicals. The radical pair polarization is created within an F-pair consisting of two partners of one and the same cyclic peptide radical species.

Acknowledgment. This work was supported in part by the Deutsche Forschungsgemeinschaft and the Graduiertenkolleg "Mechanisms and Applications of Non-Conventional Oxidation Reactions" at the University of Leipzig.

References and Notes

(1) Mee, L. K.; Adelstein, S. J. *Proc. Natl. Acad. Sci. U.S.A.* **1981**, *78*, 2194−2198.
(2) Gajewski, E.; Fuciarelli, A. F.; Dizdaroglu, M. *Int. J. Radiat. Biol.* **1988**, *54*, 445−459.
(3) Dean, R. T.; Fu, S.; Stocker, R.; Davies, M. J. *Biochem. J.* **1997**, *324*, 1−18.
(4) Wagner, A. F.; Frey, M.; Neugebauer, F. A.; Schafer, W.; Knappe, J. *Proc. Natl. Acad. Sci. U.S.A.* **1992**, *89*, 996−1000.
(5) Burdi, D.; Aveline, B. M.; Wood, P. D.; Stubbe, J. A.; Redmond, R. W. *J. Am. Chem. Soc.* **1997**, *119*, 6457−6460.
(6) Jonsson, M.; Wayner, D. D. M.; Armstrong, D. A.; Yu, D.; Rauk, A. *J. Chem. Soc., Perkin Trans. 2* **1998**, 1967−1972.
(7) Viehe, H. G.; Janousek, Z.; Merenyi, R.; Stella, L. *Acc. Chem. Res.* **1985**, *18*, 148−154.
(8) Brocks, J. J.; Welle, F. M.; Beckhaus, H.-D.; Rüchardt, C. *Tetrahedron Lett.* **1997**, *38*, 7721−7724.
(9) Reid, D. L.; Armstrong, D. A.; Rauk, A.; von Sonntag, C. *Phys. Chem. Chem. Phys.* **2003**, *5*, 3994−3999.
(10) Rauk, A.; Yu, D.; Taylor, J.; Shustov, G. V.; Block, D. A.; Armstrong, D. A. *Biochemistry* **1999**, *18*, 9089−9096.
(11) Rauk, A.; Yu, D.; Armstrong, D. A. *J. Am. Chem. Soc.* **1998**, *120*, 8848−8855.
(12) Berkowitz, J.; Ellison, G. B.; Gutman, D. *J. Phys. Chem.* **1994**, *98*, 2744−2765.
(13) Rauk, A.; Yu, D.; Armstrong, D. A. *J. Am. Chem. Soc.* **1997**, *119*, 208−217.
(14) Adams G. E.; Boag, J. W.; Currant, J.; Michael, B. D. *Pulse Radiolysis*; Academic Press: New York, 1965; pp 131−143.
(15) Simic, M. G.; Neta, P.; Hayon, E. *J. Am. Chem. Soc.* **1970**, *92*, 4763−4768.
(16) Rao, P. S.; Hayon, E. *J. Phys. Chem.* **1975**, *79*, 109−115.
(17) Garrison, W. M. *Chem. Rev.* **1987**, *87*, 381−398.
(18) Mieden, O. J.; von Sonntag, C. *Z. Naturforsch.* **1989**, *44b*, 959−974.
(19) Paul, H.; Fischer, H. *Helv. Chim. Acta* **1971**, *54*, 485−491.
(20) Livingston, R.; Doherty, D. G.; Zeldes, H. *J. Am. Chem. Soc.* **1975**, *97*, 3198−3204.
(21) Rustgi, S. N.; Riesz, P. *Int. J. Radiat. Biol.* **1978**, *34*, 301−316.
(22) Kland-English, M.; Garrison, W. M. *Nature* **1963**, *197*, 895−897.
(23) Hayon, E.; Simic, M. *J. Am. Chem. Soc.* **1971**, *93*, 6781−6786.
(24) Taniguchi, H.; Kirino, Y. *J. Am. Chem. Soc.* **1977**, *99*, 3625−3631.
(25) Sevilla, M. D.; Fallor-Koszykowski, R. *J. Phys. Chem.* **1977**, *81*, 1198−1200.
(26) Johns, R. B.; McGregor, J. W. *Photochem. Photobiol.* **1975**, *22*, 13−17.
(27) Coyle, J. D.; Hill, R. R.; Randall, D. *Photochem. Photobiol.* **1984**, *40*, 153−159.
(28) Edward, J. T. *Research Corresp.* **1955**, *8*, 38−39.
(29) Bielinski, H.; Ciarkowski, J. *Biopolymers* **1986**, *25*, 795−809.
(30) Sykes, B. D.; Robertson, E. B.; Dunford, H. B.; Konasewich, D. *Biochemistry* **1966**, *5*, 697−701.
(31) Hakin, A. W.; Kowalchuck, M. G.; Liu, J. L.; Marriott, R. A. *J. Solution Chem.* **2000**, *29*, 131−151.
(32) Hakin, A. W.; Liu, J. L.; O'Shea, M.; Zorzetti, B. *Phys. Chem. Chem. Phys.* **2003**, *5*, 2653−2657.
(33) Prasad, C. *Peptides* **1995**, *16*, 151−164.
(34) McCleland, K.; Milne, P. J.; Lucieto, F. R.; Frost, C.; Brauns, S. C.; Van, De Venter, M.; Du, Plesis, J.; Dyason, K. *J. Pharm. Pharmacol.* **2004**, *56*, 1143−1153.
(35) Fdhila, F.; Vazquez, V.; Sanchez, J. L.; Riguera, R. *J. Nat. Prod.* **2003**, *66*, 1299−1301.
(36) Mieden, O. J.; Schuchmann, M. N.; von Sonntag, C. *J. Phys. Chem.* **1993**, *97*, 3783−3790.

(37) Mieden, O. J.; von Sonntag, C. *J. Chem. Soc., Perkin Trans. 2* **1989**, 2071−2078.
(38) Reid, D. L.; Armstrong, D. A.; Rauk, A.; Nese, C.; Schuchmann, M. N.; Westhoff, U.; von Sonntag, C. *Phys. Chem. Chem. Phys.* **2003**, *5*, 3278−3288.
(39) Walling, C. *Free Radicals in Solution*; John Wiley and Sons, Inc.: New York, 1957.
(40) Loeff, I.; Rabani, J.; Treinin, A.; Linschitz, H. *J. Am. Chem. Soc.* **1993**, *115*, 8933−8942.
(41) Säuberlich, J.; Brede, O.; Beckert, D. *J. Phys. Chem. A.* **1997**, *101*, 5659−5665.
(42) Kausche, T.; Säuberlich, J.; Trobitzsch, E.; Beckert, D.; Dinse, K. P. *Chem. Phys.* **1996**, *208*, 375−390.
(43) Stephenson, D. S. *Nucl. Magn. Reson. Spectrosc.* **1988**, *20*, 515.
(44) Säuberlich, J. Ph.D. Dissertation, University of Leipzig, 1996.
(45) Geimer, J. Ph.D. Dissertation, University of Leipzig, 1999.
(46) Kirino, Y.; Taniguchi, H. *J. Am. Chem. Soc.* **1976**, *98*, 5089−5096.
(47) Wardman, P. *J. Phys. Chem. Ref. Data* **1989**, *18*, 1637.
(48) Neta, P.; Huie, R. E.; Ross, A. B. *J. Phys. Chem. Ref. Data* **1988**, *17*, 1027−1284.
(49) Huie, R. E.; Clifton, C. L. *Int. J. Chem. Kinet.* **1989**, *21*, 611−619.
(50) NIST *Standard Reference Database Number 69*, June 2005 Release. http://webbook.nist.gov/chemistry/ie-ser.html, 2005.
(51) Tarábek, P.; Bonifačić, M.; Beckert, D. *J. Phys. Chem. A* **2006**, *110*, 7293−7302.
(52) Hayon, E.; Treinin, A.; Wilf, J. *J. Am. Chem. Soc.* **1972**, *94*, 47−57.
(53) Geimer, J.; Beckert, D. *Appl. Magn. Reson.* **2000**, *18*, 505−513.
(54) Kolthoff, I. M.; Miller, I. K. *J. Am. Chem. Soc.* **1951**, *73*, 3055−3059.
(55) Tsao, M. S.; Wilmarth, W. K. *J. Phys. Chem.* **1959**, *63*, 346−353.
(56) Dogliotti, L.; Hayon, E. *J. Phys. Chem.* **1967**, *71*, 2511−2516.
(57) Chawla, O. P.; Fessenden, R. W. *J. Phys. Chem.* **1975**, *79*, 2693−2700.
(58) Muus, L. T.; Atkins, P. W.; McLauchlan, K. A.; Pedersen, J. B. *Chemically Induced Magnetic Polarization*; D. Reidel Publishing Company: Dordrecht, 1977; pp 1−407.
(59) McLauchlan, K. A.; Simpson, N. J. K.; Smith, P. D. *Res. Chem. Intermed.* **1991**, *16*, 141−163.
(60) McLauchlan, K. A. In *Continuous-Wave Transient Electron Spin Resonance, Modern Pulsed and Continuous-Wave Electron Spin Resonance*; Kevan, L., Bowman, M. K., Eds.; John Wiley and Sons, Inc.: New York, 1990; pp 285−364.
(61) McLauchlan K. A.; Yeung, M. T. *Time-Resolved ESR Studies of Free Radicals, Specialist Periodical Reports, Electron Spin Resonance, Vol. 14*; The Royal Society of Chemistry: Cambridge, U.K., 1994; pp 32−62.
(62) Verma, N. C.; Fessenden, R. W. *J. Chem. Phys.* **1976**, *65*, 2139−2155.
(63) Woodward, J. R.; Lin, T. S.; Sakaguchi, Y.; Hayashi, H. *J. Phys. Chem. A* **2000**, *104*, 557−561.